Open Access

Stechnolock Radiology and Imaging

REVIEW ARTICLE

Polymer Composites with Additives from Carbon Nanomaterials for Radioprotective Coatings

AA Babaev*

Amirkhanov Institute of Physics, Dagestan Federal Research Center, Russian Academy of Sciences, Makhachkala, 367003 Russia

***Corresponding Author:** Babaev Arif, Amirkhanov Institute of Physics, Dagestan Federal Research Center, Russian Academy of Sciences, Makhachkala, 367003 Russia, Tel.: +79285841971, E-mail: babaev-arif@mail.ru

Citation: Babaev Arif (2024) Polymer Composites with Additives from Carbon Nanomaterials for Radioprotective Coatings, Stechnolock: Radiol and Imaging. 2: 1-20

Abstract

The present brief review presents the results of studies of the electrical conductivity and microwave properties of polymer composites based on Taunite-M and shungite for production of radiation-protective coatings. Anomalies in the behavior of the electrical conductivity of the composite at a concentration of Taunite-M of ≈5.0% have been found. The following results and conclusions have been provided: 1- a technology for producing Taunite-M, which can be introduced in an amount of up to 90 wt % to a selected polymer– styrene–butadiene latex; 2- structural and optical properties of Taunite-M; 3- techniques for studying dried layers and microwave properties; and 4- drying kinetics, morphology, and relief of the composite layers. It has been established that polymer composites based on paint materials with Taunite-M can be produced as protective coatings with a 80–90% content of carbon nanoparticles.

Introduction

Radio-absorbing materials (RAMs) are designed to dissipate electromagnetic radiation (EMR) incident on them at a minimum level of reflection, which enables one to solve a variety of tasks, ranging from the absorption of "parasitic" radiation inside high--frequency units of various devices to reduction of the radar visibility not only of military equipment, but different fields of medicine. Individual pro-tection of personnel at performing various types of works under the conditions of high frequency EMR is the task of particular importance. Depending on the frequency, EMR has a different depth of penetration into different materials. The response of living organ- isms to the impact of EMR of different frequency ranges is not the same. It is assumed that the strongest response of human and animal bodies is caused by the electromagnetic field (EMF) and EMR when their frequency coincides with that of the parametric resonance of individual body systems. An EMR of centimeter and millimeter wavelengths affects mainly the human skin, whereas a decimeter EMR penetrates down to a depth of 10–15 cm, thus directly affecting the internal organs [1]. Depending on the frequency range, which is usually determined by the coefficient of reflection of electromagnetic waves, RAMs are divided into wide-range and resonant ones.

According to their structural features, RAMs are divided into single-layer, interference, gradient, and combined ones. Sin-

gle-layer RAMs, which have a uniform thick- ness structure and exhibit dielectric and magnetic properties, are narrow-band and provide effective absorption of electromagnetic radiation at a thickness equal to a quarter of a wavelength.

In terms of structure, interference radio-absorbing materials consist of a substrate and alternating dielectric and conductive layers. A dielectric layer, which is a binder, contains an absorber (for example, Fe oxides), whereas a conductive layer contains a metallized fiber.

Gradient radio-absorbing materials are characterized by a multilayer structure that provides a preset change in the dielectric constant over the thickness of a material. The outer layer is made of a solid dielectric of dielectric permittivity c proximate to 1 (e.g., pheno- lic plastic hardened with silica glass fiber). The deeper layers are made of dielectrics with higher dielectric constant - c (for example, epoxy resin with c = 5 or the same resin with a filler with c = 25) and a powder– absorber (for example, graphite dust). The described structure promotes the minimal reflection of radio waves from a surface and increases their absorption as they penetrate deep into a material [2].

The complex mechanism of electromagnetic wave propagation and EMR absorption, as well as the technological difficulties in synthesizing materials with predetermined electromagnetic properties in a wide frequency range, has resulted in a versatility of existing shielding materials and coatings. The absorption of electromagnetic energy occurs due to dielectric and magnetic losses, as well as conduction ones, which researchers try to maximize in order to achieve the maximum efficiency of the shielding effect. Thermo- plastic RAMs for use as radio shields have been developed on the basis of polycarbonates, polyamides, polypropylene, and polyvinyl chloride. Flakes of aluminum, glass, carbon, including metallized ones, metal fibers, and soot are used as fillers [3].

The properties of solidified polymers for composite materials and a number of dispersed fillers were described in [4]. Fillers are subject to a number of general and special requirements, compliance with which enables one to provide polymer composites with the necessary properties. General requirements include high wetting by a polymer material, low cost, chemical and thermal resistance, good dispersibility in a polymer, and nontoxicity.

Over the recent years, information on the possible effect of nanostructuring on the radiation resistance of materials has appeared in published studies and is being extensively discussed. It is known from this that a nanostructured material will be more resistant to ionizing radiation than a microstructured one.

Carbon nanotubes (CNTs) have a number of remarkable qualities, while being objects of nanometer scale. They conduct electric current and heat well and are strong and resistant to mechanical and temperature effects. However, it seems rather difficult to work with individual carbon tubes due to their small size and strong interaction with electric and magnetic fields. It is possible to avoid such difficulties through creating macroscopic materials based on CNTs. For instance, CNTs can be used to fabricate paper in which they are used instead of cellulose fibers. In the works published in English, such a material is called “buckypaper.” Here, CNTs are combined into bundles by the forces of intermolecular van der Waals attraction and form a stable self--supporting material due to interweaving of CNT bundles and individual CNTs, which retains a number of their characteristics. Such CNT films, as well as CNT-containing composites, are of particular interest for creating highly efficient and inexpensive systems for protection against microwave EMR. First of all, this applies to the back- ground of electromagnetic interference caused by the widespread use of mobile phones, microwave ovens, computers, etc. To protect electronic equipment in commercial applications, materials are required with a shielding efficiency above 30 dB (due to reflection, absorption, and interference quenching). Materials with significantly higher EMR shielding effectiveness—from 80 to 100 dB—are required for application in the defense industry.

The introduction of certain concentrations of car- bon nanomaterials (CNMs) into a selected polymer film-forming matrix, in principle, could result in a high-tech composite ultrahigh (microwave)-frequency absorbing material that is resistant to different external conditions.

The authors of [5] investigated the problems of studying the electrophysical characteristics of more than 250 composite materials obtained as a result of the introduction of CNTs into a polymer matrix, mainly in amounts from 0.001 to 10%. The mechanism of electron transport between CNTs with different chirality was investigated in [6]. The authors of [7] stated that the distribution of distances between nanotubes at the contact points is not uniform. The penetration of a single polymer layer between fillers reduces the contact resistance almost to the value of the resistance between nanotubes located at the van der Waals distance (3.4 Å) from each other [8]. The authors of [9–13] investigated the electrophysical properties—those of [14–20] investigated properties under a pressure of 9 GPa during compression and decompression, while the authors of [21–25] investigated the thermophysical properties of a polymer composite with high content of multiwalled CNTs of 95%, in which a 5% fluoroplastic lacquer was used as a polymer. The results of the study on the heat capacity and thermal diffusion of a polymer composite based on a large number of multiwalled CNTs in the range of 300 K 450 K were obtained for the first time. The observed maxima of heat capacity and thermal diffusion were similar to the resistance maxima found earlier in this temperature range. The hystereses of the behavior of the heat capacity and thermal diffusion in the process of heating and cooling of the composite were revealed. The detected anomalies are responsible for structural first-order phase transitions. These comprehensive studies of physical properties were carried out on a composite with 95% / 5% by weight (CNT / polymer) obtained by directional spinning. Electro- physical and thermophysical properties, elasticity, and resilience are important when creating composites for radioprotective coatings.

Various methods of modifying CNMs are used to increase the efficiency of EMR absorption: many of them involve the introduction of substances of various nature (metals, alloys, oxides, and salts) onto the sur- face or into the internal cavities of the CNM (if they exist and are available). Such methods of modification are aimed at changing the electrophysical properties of CNMs; however, not only the parameters of nanoparticles, but also the nature of their distribution in a polymer matrix have a significant effect on the properties of the studied composites. Initial CNMs are usually unevenly distributed in the polymer matrix due to their tendency to aggregation. To achieve a more uniform distribution in the polymer matrix, chemical modification (functionalization) of CNM is extensively used with the formation of functional groups on the surface, for example, carboxylic groups. However, the effect of CNM functionalization on the radio- absorbing properties of polymer nanocomposites based on them have not been properly studied. Interest in the work in the field of EMR absorption by materials containing CNM was expressed in [26], which presents comprehensive experimental data and the most important theoretical justifications.

Here, in [26], the experimental values were provided for the real and apparent components of the dielectric permittivity of the composites with CNTs in polymethyl methacrylate and polyaniline, both frequency and concentrations dependences in the range from 8 to 12 GHz were determined. In most studies, rather little attention was paid to the reflection of the microwave signal from composites in the far field, although the latter is of great importance for both basic and applied research. Moreover, it can be supposed that, as concerns the potential applicability of such composite materials for solving practical tasks many studies on the subject are classified, for which reason a large amount of published works are unavailable. In our country, such studies, as far as we know, are only starting to be developed [27, 28].

It is noteworthy that, in most composites, there is no obvious correlation between the dc conductivity and the high-frequency permittivity, when the con- centration of the nanocarbon phase varies, which allows finding the optimum in the agreed requirements for conductivity and microwave absorption. This is important, since, in conductive composites with low resistance located in the near zone of the transmitter, high RF currents can be induced, which can heat them up to temperatures at which the polymers begin to deteriorate. On the other hand, in other applications, it may be necessary to heat the coatings, which requires a certain nonzero electrical conductivity.

To create composite materials containing nanoscale carbon formations, it seems appropriate to use inexpensive materials available in large quantities. Such materials include industrially produced multi- wall CNTs (Taunite modified in various ways), functionalized materials based on them, and shungite containing fullerenes and a number of impurities. The purpose of this work is to create and study various composites with additives of carbon nanoparticles for maximum radiation protection coat-

ings. Various composites have been studied, where various polymers were used as a matrix This review provides a brief study of the approaches used in researches, with a particular focus on polymer composites based on Taunite-M carbon materials and shungite, which can be introduced into the polymer in large amounts. The polymer butadiene styrene latex is of particular interest, since a uniformly large amount of nanoparticle filler up to 90% wt. % can be introduced into this matrix. This can lead to the creation of composites that can be used in various industrial applications by changing the physical properties within wider limits

Synthesis Technology for Taunite-M, Properties of Shungite

CNTs of the Taunite series are fabricated in NanoTechCenter LLC based on the CVD technology. A powdered catalyst is loaded into a reactor and brought into contact with hydrocarbons, which serve as a source of carbon. A propane-butane mixture is used as a source of hydrocarbons. The process is carried out in certain modes (temperature 600–700^{0}C, preset ratio and gas components feed rate), which are monitored by the control system. The structure of the resulting nanotubes is mainly determined by the catalyst used, which comprises oxide systems containing catalytically active metals (iron, nickel, cobalt, and molybdenum) and an oxide matrix with a developed surface (magnesium and aluminum oxides). Taunite CNTs are produced on a nickel-containing catalyst with a conical structure of carbon layers and an internal channel. Taunite-M CNTs is produced on catalysts containing iron, cobalt, and molybdenum and has a cylindrical structure of the carbon layers. All these catalysts are developed and manufactured by NanoTechCenter LLC. The first platelike reactors with a fixed catalyst layer were created by NanoTechCenter LLC, and, after a number of improvements, they are still operated. The capacity of such a reactor is about 100–200 g of nanotubes per technological cycle, depending on the catalyst used and the growth time. Short CNTs of the Taunite-M type with a short growth time (5 min) are of particular interest. Such CNTs are less agglomerated and better distributed in different media.

For better compatibility with polar and nonpolar matrices, NanoTechCenter LLC develops experimental batches of CNTs, the surface of which is functionalized by oxygen groups through oxidation (hydrophilic, for polar media) or modified by hydrocarbon groups (hydrophobic, for nonpolar media). It is also possible to fabricate CNTs modified by other ways (by phenol–-formaldehyde oligomers, sulfur, polyaniline, ferrite nanoparticles, etc.). Such modified nanotubes are of interest for certain applications (concentrated water dispersions, rubber mixtures, epoxy compositions, adsorbents, etc.).

There are various ways to produce catalysts in order to prepare CNTs. Numerous catalysts are known for the production of CNTs by the method of the catalytic pyrolysis of hydrocarbons, which are catalytically active metals, a mixture of catalytically active metals or their oxide precursors, deposited or distributed on a dispersed matrix (carrier) [29–37]. The disadvantages of the known catalysts of this group include low activity manifested in a small mass yield of carbon nanotubes per unit mass of a catalyst and low quality of the resulting nanotubes manifested in a large spread of the geometric parameters of CNTs and the presence of a large number of defects in the structure of CNTs and significant carbon impurities. To avoid these disadvantages, the authors of [38, 39] synthesized new catalysts for the production of carbon nanotubes by the method of catalytic pyrolysis of hydrocarbons. The catalytic pyrolysis of hydrocarbons entails a process in which the thermal decomposition of a hydrocarbon (for example, methane, propane, butane, ethylene, propylene, acetylene, benzene, and xylene) occurs on the particles of a solid catalyst, resulting in the formation of carbon in the form of nanofiber or nanotubes. Metal oxide catalysts for growing carbon nanotubes from the gas phase containing a transition metal com- pound and more than one phase of aluminum and magnesium oxide compounds were described. As a transition metal compound, the catalyst contains two or three metals selected from the group (iron, cobalt, and molybdenum), whereas the ratio of a transition metal atoms contained in the catalyst in greater amount to the sum of the transition metal atoms contained in the catalyst in smaller amount is from 1 : 0.1 to 1 : 0.805. The atomic ratio of the sum of transition metals to the sum of aluminum and magnesium in the catalysts is from 0.02 to 1.5, while the atomic ratio of magnesium to the sum of aluminum and magnesium in the catalysts is from 0.1 to 0.95. The technical result is that the use of the described catalyst provides a high yield of high-quality carbon nanotubes and entails the use of cheap initial hydrocarbon materials. To prepare polymer nanocomposite materials, a Taunite-M car- bon nanomaterial comprising a

multiwalled CNT with a diameter of 10 to 30 nm and a length of more than 2 μm was used (Figure 1).

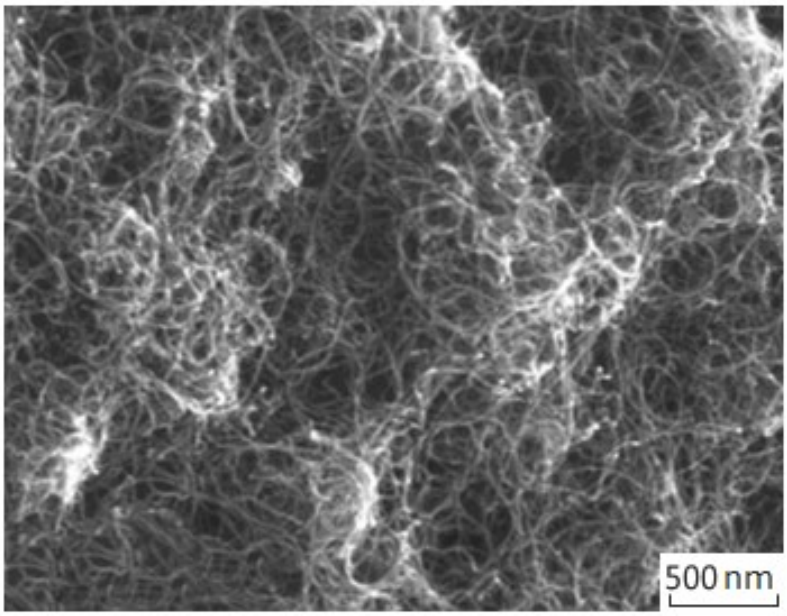

Figure 1: Taunite-M carbon nanomaterial produced by Nano- TechCenter LLC (Tambov).

The unique natural material shungite was used in the polymer composites. Shungite consists of carbon, a part of which consists of spherical molecules – fullerenes. Shungite, also known as carbon black, lydite, paragon, or fullerite, is a Precambrian rock that is between anthracite and graphite in terms of composition and properties. Shungite carbon forms a matrix in the rock, in which dispersed silicates are evenly distributed. A fullerene molecule is an organic molecule. A crystal formed by such molecules (fullerite) is a molecular crystal that is the link between organic and inorganic matter. The interest in using shungite as a filler is determined by the presence of noncrystalline carbon and silicon dioxide in its composition—two components that are chemically similar to technical carbon (TC) and dioxide (white soot). The mineral and carbon components of shungite are not chemically related to each other, they do not separate even when shungite is dispersed to a size of ≈1 μm, and they have the ability to be introduced into almost all polar and nonpolar polymers. Shungite is prepared for use as a filler by grinding shungite rocks from Karelia, Russia. The size of the main particle fraction is 2–8 μm. The introduction of the filler changes the morphology of the polymer, its crystallinity degree in particular. The effect of shungite on the properties of polymer com- posite (PC) and its use have been studied by many authors [40–46]. Shungite is normally used instead of TC, which leads to an increase in plasticity and an improvement in the recyclability of PC. Shungite can be also considered as a reinforcing filler, while the amount of its introduction results in values comparable to those for TC, much less (a fraction of a percent compared to tens for TC), which is explained by the presence of fullerenes in shungite.

Structural and Optical Properties of Multiwalled Carbon Nanotubes

Taunite is produced by the catalytic pyrolysis of methane on a specially prepared substrate with a catalyst (nickel) deposited on it in the form of a fine pow-der. Two products were studied: one produced directly from the reactor and the purified one, mostly from the nickel impurity, by treating it with nitric acid. The ash content of CNT was ~1%, mainly due to the residual nickel content [47]. In the end sections of the chevron- type carbon fiber, metal particles were identified, the origin of which was explained by the capturing of catalyst particles during the synthesis [48]. A mixture of two types of CNTs, parallel and chevron, causes significant difficulties in terms of both determining their relative content and the physical separation of CNTs on the structure type. For macroscopic quantities of CNTs, no methods have been developed so far to solve this task in any effective way. CNTs were characterized by means of the Raman spectroscopy and microscopy [49, 50]. Figure 2 shows one of the characteristic pairs of the spectra. Peaks in the range of 1320–1340 cm^{-1} are usually associated with the diamond sp3 phase (the exact value for diamond is 1332 cm^{-1}); however, one should bear in mind that pyrolytic graphite has a proximate peak at 1355 cm^{-1}.

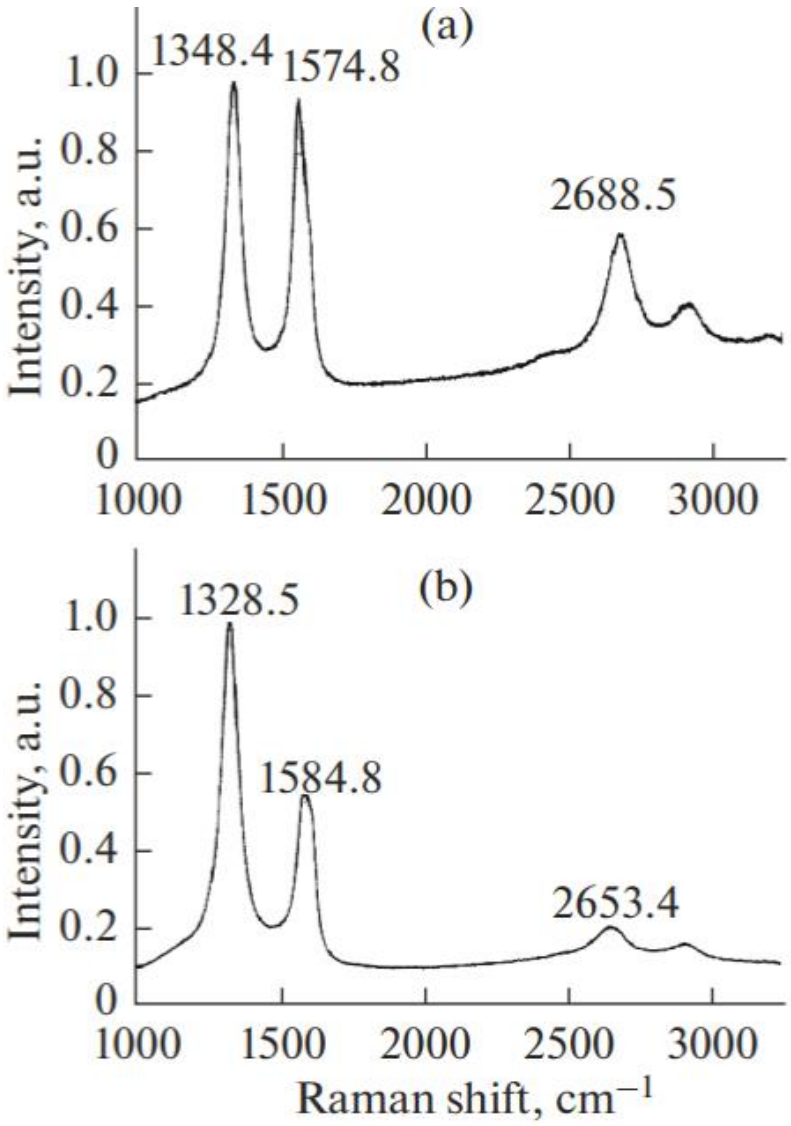

Figure 2: Micro-Raman spectroscopy of CNTs. Dispersion of the spectra under excitation λ = (a) 0.514 and (b) 0.63 μm.

Based on the dispersion parameters, it can be established that the observed line corresponds particularly to nanographite rather than to the diamond phase. This is also corroborated by the presence of a strong band at 1574–1584 cm^{-1}, since both single-crystal and pyrolytic graphite have a peak at 1580 cm^{-1} [51]. Optical spectroscopy in the visible and near-UV regions enables one to estimate the electron work function from CNTs. The obtained spectra are characterized by an intense peak corresponding to an energy of about 5.0 eV, as well as several less intense peaks of lower energy. These peaks are presumably caused by structural defects, the nature of which is not yet clear. Figure 3 shows the absorption spectrum of CNTs at room temperature.

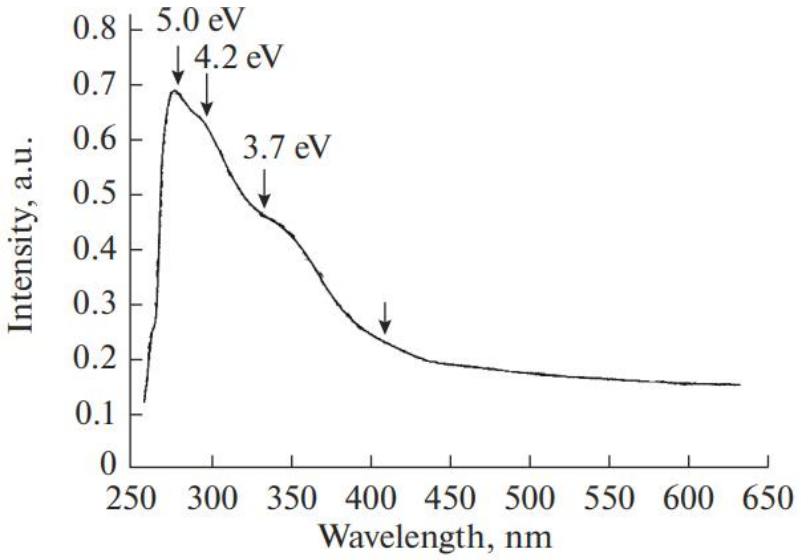

Figure 3: Absorption spectrum of CNTs.

For energies above 5.0 eV, there is a noticeable decrease in the absorption intensity. Such values of the work function of carbon structures are typical for both graphite and diamond. The aggregation of carbon nanofiber (CNF) on a macroscopic scale is of particular interest. A CNT water dispersion was introduced into the space between two plane-parallel glass plates with a gap of approximately 70 μm, with the side walls closed to prevent water evaporation. The same surfactants were added to the water in the same concentration that were used in the preparation of the composite based on styrene–butadiene latex. Five days later, the complete adsorption of water by nanofibers was observed, which, as the water was absorbed, formed a figure of a pronounced fractal shape (Figure 4).

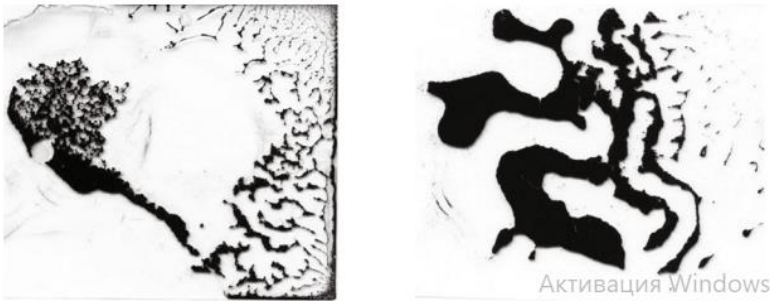

Figure 4: Macroscopic self-organization of CNTs: frame size 29 × 25 mm. On the left is the frontal dimension of the fragment contour.

Water is intensely adsorbed (with surfactants) in an enclosed volume on the CNT surface, whereas the CNT is simultaneously organized into a complex branched structure. For polymer composites, a rather high water content directly on the branched surface of the carbon core must be essential.

Polymers and Carbon Materials

The selection of a polymer for the preparation of composites based on CNM requires a preliminary task statement. For applications in which high thermal, chemical, plasma, and radiation resistance is required, poly(o-hydroxy amides) are the optimal solution. For most practical applications in atmospheric conditions, poly(styrene–butadiene) is more efficient; moreover, it is an environmentally friendly polymer, one of the synthetic analogues of natural rubber. Latexes are inexpensive materials among substances that can effectively form a matrix for introducing nanocarbon into it and eventually produce latex paints, in the formulation of which CNM will replace or play the role of a dying agent.

Polypyrrole, despite all the described practical difficulties, is of theoretical interest, since it enables one to reveal more deeply the nature of the interactions between polymer and CNM. From a practical point of view, such composites have no potential,

since “soluble” polypyrrole is an unstable “exotic” product.

Epoxy matrices do not provide an acceptable level of electrical conductivity and microwave absorption. The introduction of CNM into them is of significant interest only from the point of view of modifying the mechanical, plastic, and tribological properties of cured epoxy resins.

The following materials were used to prepare composites as polymer matrices.

— Butadiene–styrene latex and composites based prepared according to the technology used in the advanced paint and lacquer industry. CNM and styrene–butadiene latex were introduced into the composite, as well as surfactants (surface-active substances), coalescence agents homogenizing the resulting mixture, and defoamers. The solvent here is water. The layers are formed when the liquid phase is dried.

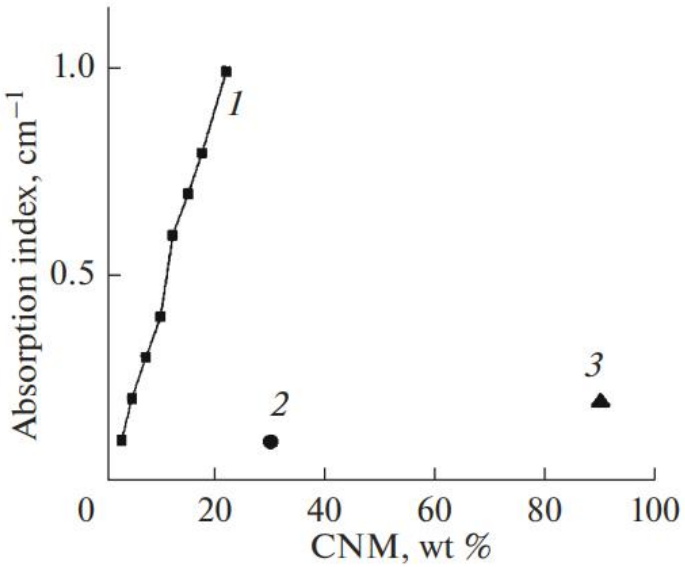

Figure 5: Absorption indices of the protective coatings with a thickness of 200 μm based on the modified CNTs (*1*) PANI-CNT, (*2*) CCNT, and (*3*) EF-CNT.

- *Soluble polypyrrole* created according to the tech- nique described in [7]. The solvent here is chloroform. The solid phase is obtained by evaporation of the sol- vent at room temperature or with heating up to 70– 150^{0}C.

- *Poly(o-hydroxyamides)* synthesized at the Insti- tute of Macromolecular Compounds of the Russian Academy of Sciences. The solid phase was produced by drying the composite lacquer at a temperature of 95C. When the polymer is thermally pretanned up to a temperature of 350^{0}C, poly(*o*-hydroxyamide) is converted into polybenzoxazole and, consequently, the physical properties of the polymer matrix are radically changed.

The following materials were used as carbon-containing fillers.

- *Carboxylated CNTs (CCNTs).* The use of CCNTs in the form of a 10% water paste proved difficult. This paste comprises not a homogeneous pigment bulk, but shapeless, slightly moistened lumps of different sizes, the addition of which to the paint composition did not allow producing a homogeneous liquid phase similar to paint. It was possible to add only a maximum of 30% of such a “paste” to the created composition, which resulted in an inhomogeneous and very thick bulk not suitable for applying a coating of a homogeneous quality to the glass. Therefore, considering the percentage of carbon particles in the initial water paste, the maximum content of CCNTs in the achieved protective layer was only 3 wt %.

- *Polyaniline-modified CNTs (PANI-CNTs).* A PANI-CNT (60% polyaniline) comprises a micro- dispersed homogeneous powder convenient for intro duction into an anti-corrosion paint composition, in which, in addition to the film-forming agent (s-

tyrene–butadiene latex) and anti-corrosion pigment (zinc phosphate), only the test sample is included, without foreign fillers. The introduction of PANI- CNTs into the polymer leads to a rapid increase of the viscosity of the composition, which did not allow the introduction of more than 22 wt % of this powder into the polymer composition. Here, the CNT content in the resulting coating did not exceed 8.8%.

Superconcentrate of CNTs in epoxy/formaldehyde resins (EF-CNTs). An amount of 20% concentrate of EF-CNTs could not be introduced directly into the rene–butadiene latex were introduced into the composite, as well as surfactants (surface-active substances), coalescence agents homogenizing the resuling mixture, and defoamers. The solvent here is water. The layers are formed when the liquid phase is dried7

The following materials were used as carbon-con- taining fillers.

- Carboxylated CNTs (CCNTs). The use of CCNTs in the form of a 10% water paste proved difficult. This paste comprises not a homogeneous pigment bulk, but shapeless, slightly moistened lumps of different sizes, the addition of which to the paint composition did not allow producing a homogeneous liquid phase similar to paint. It was possible to add only a maximum of 30% of such a "paste" to the created composition, which resulted in an inhomogeneous and very thick bulk not suitable for applying a coating of a homogeneous quality to the glass. Therefore, considering the percentage of carbon particles in the initial water paste, the maximum content of CCNTs in the achieved protective layer was only 3 wt %.

- Polyaniline-modified CNTs (PANI-CNTs). A PANI-CNT (60% polyaniline) comprises a micro- dispersed homogeneous powder convenient for intro-paint composition, so that EF-CNTs were used as a solution of this condensate in chloroform (content 13.8 wt %). Polyethylene polyamine (PEPA)—a com- mon industrial hardener for epoxy resins—was used as a hardener. An amount of 10 wt % of PEPA was added to the solution in chloroform and was applied after stirring to the glass plates by the pouring method. The curing was carried out after chloroform volatilization at a temperature of 80⊠C for 3 h. The result was homogeneous solid coatings with a CNT content of about 11%.

- Shungite (Karelian deposits) as a carbon-containing material.

Layers containing PANI-CNTs are characterized by a relatively high concentration and more uniform distribution of CNT in bulk and nonzero, albeit low, microwave absorption capacity (Figs. 5, 6), which confirms the necessity to increase the concentration of CNT particles in protective coatings, if one wants to achieve significant results (from the practical point of view) [52].

Based on the presented CNT modifications (CCNT, EF-CNT, PANI-CNT), it is not possible to achieve a noticeable increase of the concentration of carbon nanoparticles in the resulting composite layers due to low initial content of carbon particles in the initial components.

A series of composites with different component ratios were prepared for those combinations of the car- bon filler and the polymer matrix, which were not excluded. This allowed further building the concentration dependences of a number of parameters for composite films.

Methods for the Study of Dried Layers and Microwave Properties

The heterogeneity of the surface relief of the samples was studied both on a microscopic level and with statistical averaging over an area of more than 1 cm2. The dried composite layer underwent high-resolution optical scanning over an area of 4 cm2; the square of the modulus of the two-dimensional derivative of the image brightness value (characterizing the relative height of the relief) was then calculated for the resulting array of graphic data at each point and then aver- aged over the entire area with the calculation of the arithmetic mean and variance. For the CNM samples in styrene–butadiene latex, this parameter was de- ter-mined as a function of the concentration of CNM.

A study of microwave absorption and reflection from the surface composite layers was performed on an installation in which the operating frequency of the generator was varied in the range of 38–43 GHz. The radiator had a slot configuration; the sample was mounted in the far field of the electromagnetic wave on the movable console with an electric drive. The amplitude of the transmitted and reflected waves was recorded using two horn antennas. The slot emitter was built into a complex resonator design, which allowed providing optimal conditions for the wave formation. The microwave signal was modulated by rectangular pulses with a repetition frequency of 2–5 kHz, and, accordingly, frequency-selective Unipan voltmeters were used that were equipped with inputs for the sync signal, which provided an increased stability of their phase detectors. The spatial movement of the sample relative to the statically fixed emitter and receiving antennas allows scanning the surface and, with proper analytical processing, obtaining information about the uniformity of the spatial distribution of the values of microwave absorption and reflection over the sample area. This technique also allows providing a more accurate esti- mate of the integral parameters averaged over the entire sample. The presence of an automated drive, as well as automatic taking of instrument readings and recording them in a file on a PC connected with the measuring unit, eliminates the need for an operator during the measurements. This significantly improves the interference protection of the system and reduces the noise level substantially. An ADC manufactured by the National Instruments was used for digital recording of the measured signals: it was controlled by a software model created and running in the LabView environment.

The described method is based on the approach formulated and applied in [53, 54], which also showed the efficiency level of this measurement method in the millimeter range.

A specialized technical and methodological base was formed to study the electrophysical properties of the samples. It focused on taking into account all the specific features of the studied composites. One of the important aspects is the development of substrates with a relatively complex pattern of metal contacts, on which a layer of the composite was applied and dried. The electrophysical parameters were then measured. All the substrates were made of fiberglass, foiled with a copper layer of a thickness of 40μm. A lithographic process was used to resolve parallel isolated contact strips of a width of up to 130μm and the same distance between them. Upon etching the contact pattern, all the substrates were thoroughly washed with ethanol, acetone, and distilled water. In case of long-term storage, prior to applying the samples, the copper surface was restored in a 30% HCl solution (or briefly in an aqueous solution of $FeCl_3$, since HCl is known to form during the first stages of the interaction of CuO with $FeCl_3$ in an aqueous medium), followed by washing in distilled water.

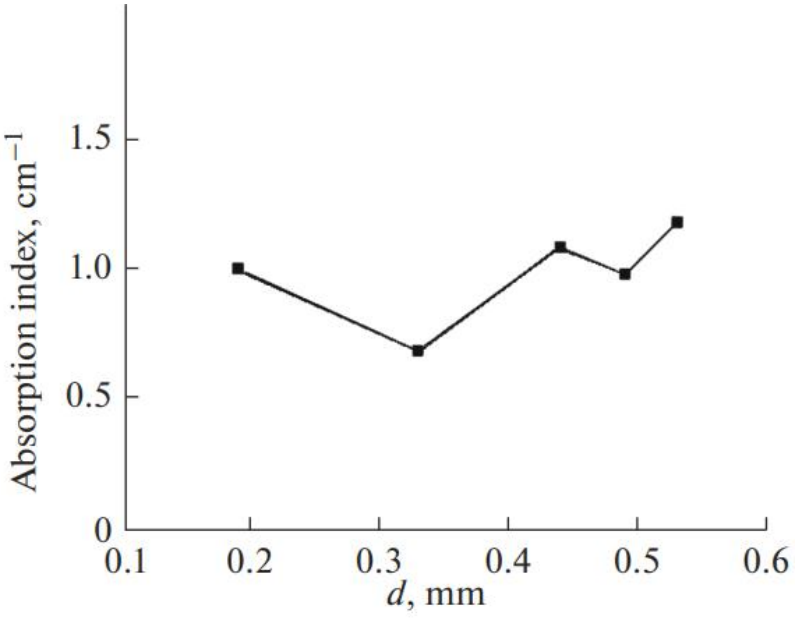

Figure 6: Dependence of the absorption index on the thickness of the protective coating. Concentration of PANI-CNT of 22 wt %.

Drying Kinetics, Morphology, and Relief of Composite Layers

The kinetics of drying of the composite layer was studied by three methods: by controlling the weight of the sample (that is, by periodically weighing it); by controlling the conductivity via the pulse method, which prevents the electrolysis destruction of a drying layer; and optically, by microphotographing the drying layer.

Figure 7 shows the time dependence of the sample weight change due to water evaporation. Note that the point of stabilization of the sample weight on the graph is defined as the intersection of two exponential asymptotes, which approximate the initial and final sections of the curve, respectively. From the point of view of mechanical properties, it also makes sense to consider the moment of visual drying, when the entire surface of the sample is no longer specularly reflective and, having gained a rough relief, becomes diffusely reflective. This aspect corresponds to the water evaporation only from the surface of a layer, but it is the dried surface layer that holds the underlying inner layers, even if they remain semiliquid, from mechanical damage, as well as from their possible overflow at moving and turning the sample in space.

The formation of a surface layer significantly complicates further evaporation of water from the underlying layers, if there is any left. Therefore, the appearance of the surface layer should affect the evaporation kinetics, which, in fact, is observed at the indicated point in Figure 7.

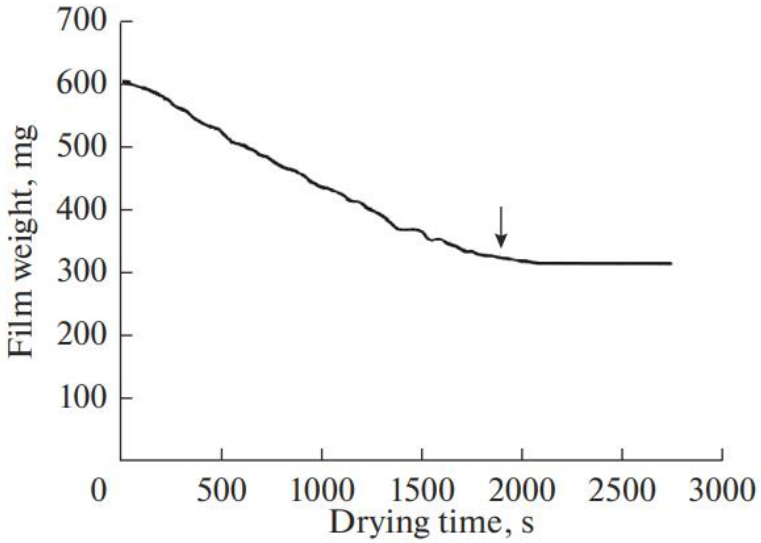

Figure 7: Change in the weight of the sample during drying.

A similar pattern is observed on the time dependence of the electrical conductivity of the layer. The corresponding graph is shown in Figure 8. Comparing this dependence with the graph in Figure 7, one can see that the decrease of the conductivity during the drying was less than 3.8-fold, while the water content decreased by weight more than 6.5-fold. From the latter one can conclude that the contribution of the electrolytic conductivity of water to the total conductivity of the dried coatings can be no more than 50–60%.

Further experiments on the removal of bound water (thermally and chemically) corroborated that the decrease of the conductivity is not more than 40– 50%, assuming the preservation of the polymer structure and the interface at its boundary with the CNF. These data correspond to the composite with a carbon nanofiber tube content of 25–30 wt % in the liquid phase and, presumably, are not reproduced in the case of noticeably lower concentrations. The stabilization of the conductivity, as well as the weight, corresponds to visual drying of a layer. The slowing down of the change in conductivity should be noted, which is associated with the slowing down of water evaporation due to the formation of a dense dried surface layer. It is of interest that the moments of time of the drying by weight and by conductivity almost coincide.

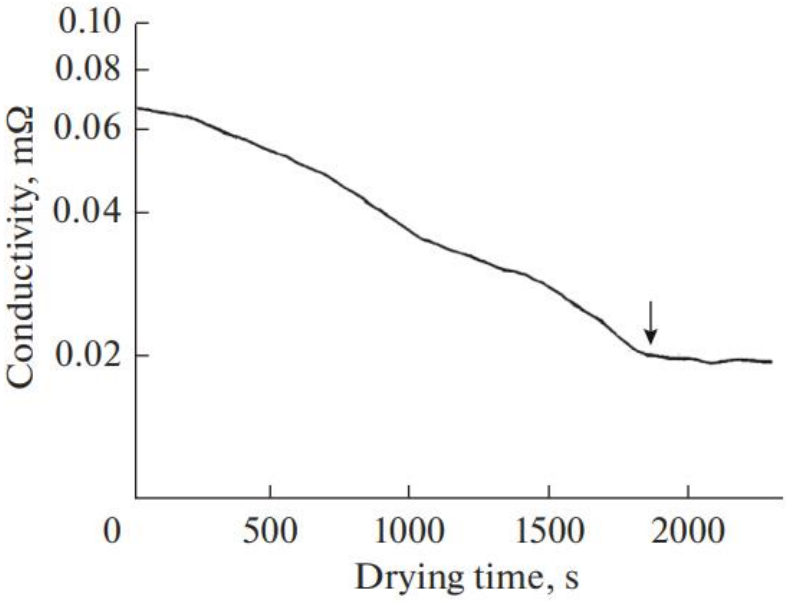

Figure 8: Changes in the conductivity of the sample during drying.

The formation of the surface dried layer does not mean that the morphology of the entire layer is completely formed, as can be seen from the analysis of the microrelief of the drying layer (Figure 9). Comparing the moment of visual drying of the layer coinciding with the point of relative stabilization of the weight and electrical conductivity of the sample, one can see that the microrelief continues to form for a noticeable time after reaching this stage. First, this could be related to the process of internal water adsorption; second, to its further, albeit slower, evaporation from the layer; and, finally, to the emergence of mechanical stresses under the dried elastic upper layer causing a reorganization of the morphological structure. In general, all these processes are accompanied by an increase of the het- erogeneity of the relief that is, despite the expectation of the formation of a smoother surface due to the elasticity of the dried latex: on the contrary, the clustering of CNTs with the formation of a network of carbon particles seems to prevail, with a complex branched pattern permeating the entire sample. It is worth mentioning that such a picture is one of the fundamental ideas of the percolation theory about the formation of a so-called "infinite cluster," which indeed permeates the entire sample and forms the skeleton of an electrically conducting network in the bulk of the dielectric medium.

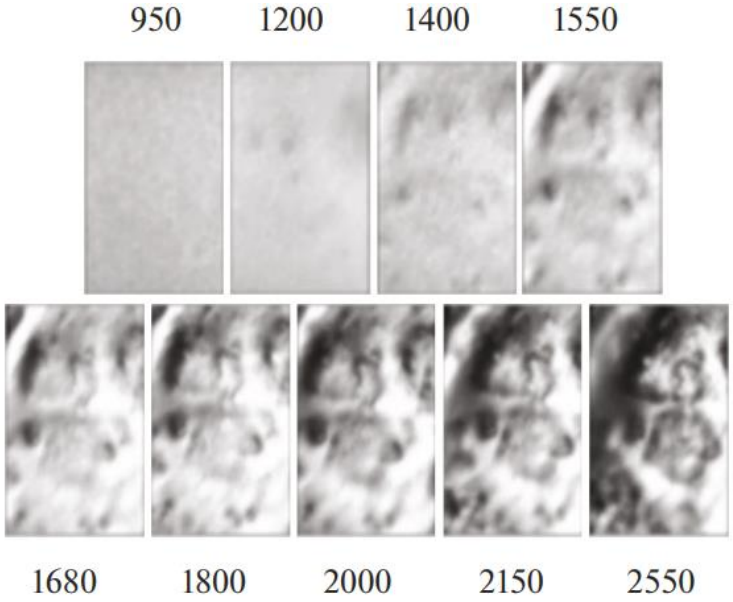

Figure 9: Formation of the relief of the dried layer of the com- posite based on CNT (frame size 75 × 100 mm; the time is counted in sec from the moment of applying the liquid layer).

For dried layers of the composites with different concentrations of CNTs, the surface morphology is most diverse on a scale of 100m–1 mm, where the most heterogeneous areas of the forming relief are located. In addition, the concentration dependence of the morphology of the layers is nonlinear and even nonmonotonic, with a pronounced extremum in the middle part. For the study, two series of composites based on CNTs and styrene–butadiene latex were created. In each of them, the concentration of CNTs varied from 8 to 35 wt % in the liquid phase. The series differed in the ratio of the content of CNTs and water (excluding water in latex), which was maintained constant for each series. Figure 10 shows images of the surfaces of the dried composite samples.

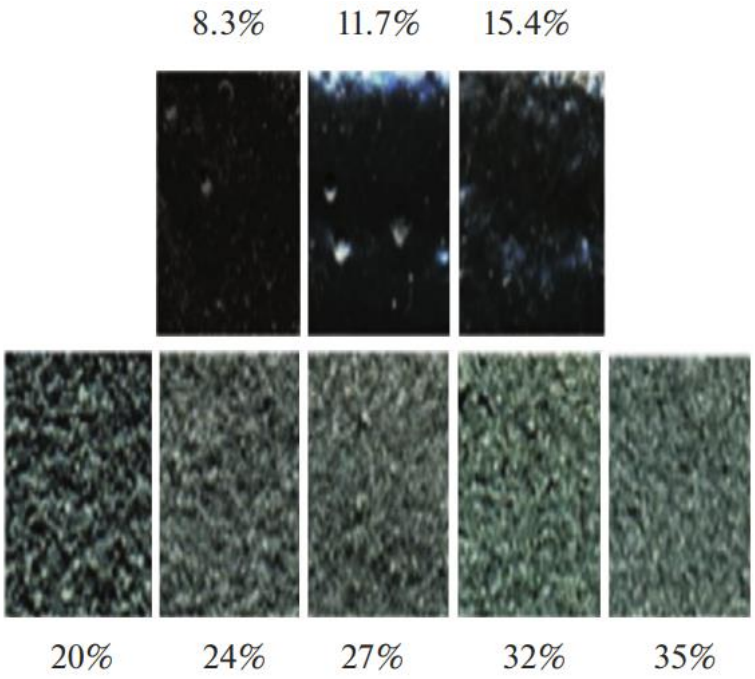

Figure 10: Relief of the dried composite layers (frame size 8 × 6 mm, CNT concentrations are shown in wt % in the liq- uid phase).

One can clearly see the emergence of a highly inhomogeneous relief near the concentration of 15–20 wt % in the liquid phase. This can be explained as the transition of CNT particles from the state with a uniform distribution over the sample volume to a highly clustered network of individual islands separated by branched "valleys." As the CNT concentration increases, the valley space gradually begins to be filled with particles that, presumably, did not join the "islands," so that the average relief becomes more homogeneous.

The transition from the homogeneous system to the highly textured one occurs in a very narrow range of concentrations and is abrupt. It was assumed that the fractal dimension of the nanocarbon network should also decrease abruptly, corresponding to the transition from an unordered three-dimensional set of "islands" to a branched two-dimensional network.

The reason for the abrupt change in the dimension is not clearly established at the moment, but it should be noted that the characteristic size of the optically distinguishable inhomogeneities of a layer corresponding to the CNT concentration of 20% is from 120 to 300 μm, which is comparable to the thickness of the layer itself. However, if there were only a simple increase in the "islands" of aggregated CNTs with increasing concentration, the transition from the 3D to the 2D structure would occur more smoothly, rather than abruptly. There must be a certain threshold at which the CNT clustering process seems to change its character significantly.

The various expressions of agglomeration and self- organization of CNTs shown above have a fundamentally important role here. It is the dynamic equilibrium of self-organization and entropy "smoothing" (caused, for example, by Brownian motion in a liquid, as well as mechanical stresses in the layer during the solvent evaporation) that leads to a noticeable change in the properties of the resulting composite layers, even with a small violation. However, without an adequate numerical model, it is diffi-

cult to reasonably judge how much the sharpness of the observed transition can correspond to the shift in the balance between the contributions of self-organization and entropy.

One can see that, in the range of 15–20%, the sur-face turns from smooth to strongly rough one with a characteristic size of inhomogeneities of 150–500m, the average value of which slowly decreases with further increase of the concentration. Increasing the number of the samples studied and applying the method described in the section (techniques for studying dried layers and microwave properties), the values corresponding to the relief intensity were obtained, as well as the value of the statistical dispersion of the relief parameter over the area of each of the samples. Both values are presented on the graph as a function of the CNT concentration, with the average relief values given as experimental points and the dispersion values as corresponding measurement errors (Figure 11).

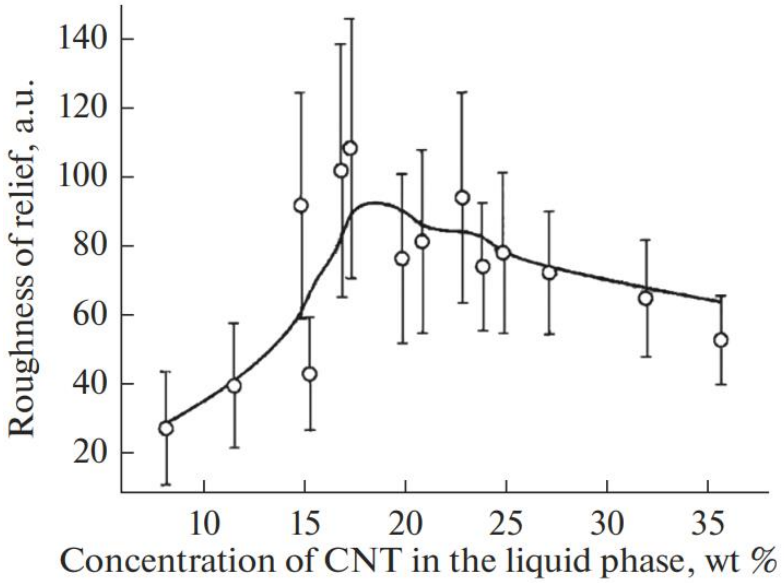

Figure 11: Concentration dependence of the inhomogeneity of the CNT composite relief in styrene–butadiene latex.

For a larger number of the samples, the dependence has a larger statistical spread. However, the pronounced abrupt transition here also corresponds to what was visually noticeable in Figure 10, especially since the experimental points near the concentrations of 15–18% do not have the intermediate values obtained by the averaging and smoothing.

Conductivity and Microwave Properties of Taunite-M Polymer Composites and Shungite

Figure 12 shows a graph of the concentration dependence of the conductivity of the samples measured at a low direct current [55–56]. The concentrations here are provided in weight percentages for the solid phase. Note that the points that are clearly out of the general trend, corresponding to a reduced conductivity in the concentration range of 43–52%, were tested repeatedly on various samples, as well as other points that were suspected to be artifacts.

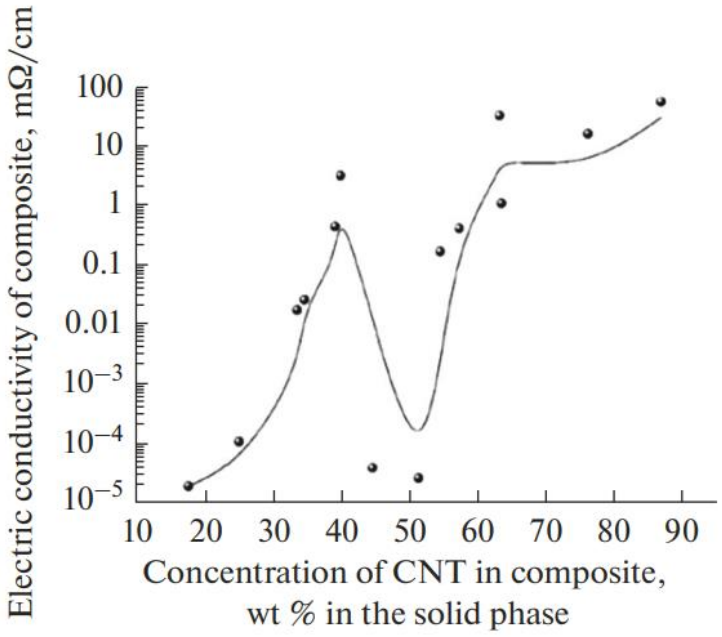

Figure 12: Concentration dependence of the electrical conductivity of the CNT composite in styrene–butadiene latex

The minimum of this dependence corresponds to the concentration at which there is an abrupt change in the morphology of the layers, the roughness of the relief, and the microwave properties. It is worth noting that, if the relief indicators change by tens of percent, the conductivity changes by several orders of magnitude. This allows it to be supposed that there is an exponential dependence of the conductivity on the spatial characteristics of the conducting structure near the critical concentration. A similar dependence is known to take place in the model of hopping conductivity. However, a more consistent explanation of the detected dependence can be provided based on the concepts of percolation theory. The phenomenon of percolation (insulator–conductor transition) for such composite heterogeneous media is difficult to describe in the framework of a strict theory based on numerous experimental studies—in particular, for polymers with additives of carbon nanotubes, graphene, black carbon, and nano- and microparticles of metals. Since the percolation model does not depend on the nature of the particles and the nature of the matrix insulator, it can be used for most polymers filled with powdered materials, such as black carbon (BC), etc. Particles of both BC and other fillers are known to be dispersed in a matrix in the form of clumps of different sizes and different geometric shapes, which vary depending on the degree of saturation with the filler. Therefore, the threshold conductivity will also depend on these characteristics of a filler. In general, both the volume concentrations of the filler typical for the percolation limit and the width of the transition insulator–conductor are determined by the size of the particle aggregates, the geometry, and the orientation (position) of the particles in the matrix. According to this theory, near the flow threshold, the conductivity increases as

$$\sigma=\sigma 0(x\text{-}xc)^{t}\text{ , at , } x\geq x_c\ \sigma = 0\text{, at , } x\prec x_c$$

where σ_0 is the conductivity at 100% of the concentration of the conducting phase (in our case, this is CNT), meaning x = 1; xc is the critical concentration corresponding to the flow threshold; and t is the critical conductivity index. It is known that, for a two-dimensional system, $x_c = 0.5$, while $x_c = 0.16$ for a three-dimensional system [57, 58]. If one reconstructs Figure 12 in linear coordinates, then the points at which the branches of the power dependence should begin that approximate the corresponding sections of the experimental curve will correspond to the values of 15–20 and 45–50%, or values of $x_c = 0.15–0.20$ and 0.45–0.50. If one translates the assumption of a uniform distribution of CNT particles in the sample bulk at their low concentrations and their clustering into large "islands" when the critical concentration is reached into the terms of percolation theory, then one should speak about a three dimensional system transforming into an ordered network of islands in all three dimensions that is comparable to the layer thickness and, therefore, limited in localization in one direction, i.e., two-dimensionally organized. Thus, the minimum conductivity at a concentration of about 50% in the solid phase can be explained by the transition

from a three- to a two-dimensional organization of the system, i.e., the transition to the stage of growth of CNT clusters in the layer at which their average size reaches an order of magnitude of the layer thickness. No theoretical model of this phenomenon was found in the published studies. Therefore, the proposed interpretation can serve as a starting point for a more detailed study of the observed effect. However, the percolation theory does not answer the question of the nature of the mechanism that causes such a dramatic change in the dimension of the CNT–polymer system. As well as the exponential dependence of the conductivity on the dimensional parameters, it tends more to the basic laws of the theory of hopping conductivity, as was stated above. However, the main provisions of this theory, which is based on a quantum mechanical model that was developed in detail for semiconductor and pure polymer systems, cannot be directly transferred to our case. It is likely that the main values here are not the distances between individual CNTs, but those between neighboring macroclusters, which are many orders of magnitude greater than the typical electron tunneling distances. Therefore, the external similarity of the dependences can, nevertheless, be hardly described by the equations obtained for systems of a fundamentally different structure. The interest in the microwave properties of CNM is quite to be expected, primarily due to the high microwave absorption in macroscopic graphite. To evaluate the properties of CNT-based composites, we compared them with similar composites based on shungite, a mineral consisting of at least 30% carbon and having no nanostructure. In addition, aluminum and silicon oxides and other compounds common to such rocks also contribute to the absorption of microwave radiation. Figure 13 shows the values of the microwave reflection coefficient from CNT and shungite samples in styrene–butadiene latex, and Figure 14 shows the microwave absorption data for the corresponding composites. Note that the concentration scale is converted to weight percentages for the solid phase. As a result, the critical concentration corresponding to a sharp change in the character of the relief, i.e., 16–18 wt % in the liquid phase, corresponds to the concentration of 45– 55 wt % in the solid phase, which is obtained by recalculating the weight fractions after deducting the water contribution.

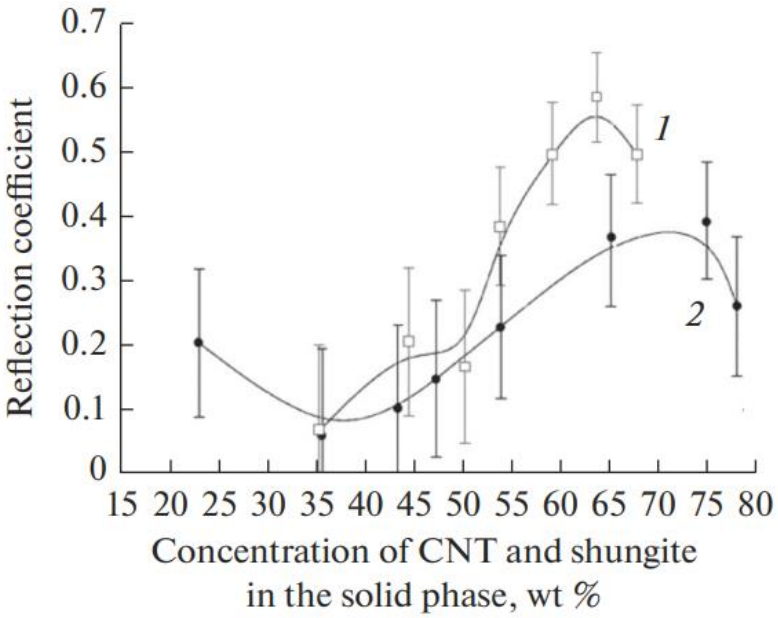

Figure 13: Microwave reflection by composite films based on (1) CNT and (2) shungite in styrene–butadiene latex.

Figure 13 shows the values of the microwave reflection coefficient from CNT and shungite samples in styrene–butadiene latex, and Figure 14 shows the microwave absorption data for the corresponding composites. Note that the concentration scale is converted to weight percentages for the solid phase. As a result, the critical concentration corresponding to a sharp change in the character of the relief, i.e., 16–18 wt % in the liquid phase, corresponds to the concentration of 45–55 wt % in the solid phase, which is obtained by recalculating the weight fractions after deducting the water contribution. The curves in Figs. 13 and 14 corresponding to the CNT composite in poly(styrene–butadiene) have not very pronounced, but still noticeable, bend points, both in the reflection and absorption at the concentration close to the critical one. This effect was not observed for the composite based on shungite. This shows that the morphology of composite films affects their microwave parameters, despite the fact that the spatial parameter of the inhomogeneity of the relief of all the samples is less than 5% of the wavelength of microwave radia-

tion. This means that the morphology affects the microwave properties not directly, but indirectly, for example, by modulating the high-frequency conductivity, which, in turn, is reflected in the absorption index. The change in morphology presumably indicates a change in the structure of the composite due to the crystallinity of the polymer.

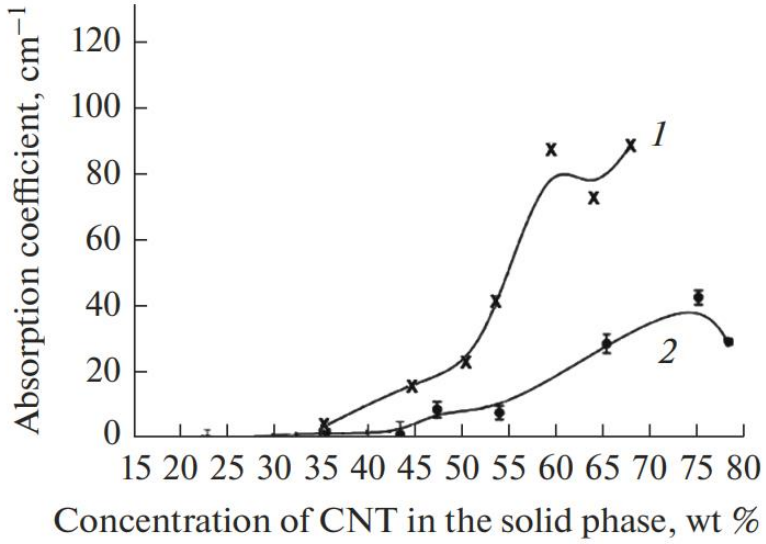

Figure 14: Microwave absorption by composite films based on (1) CNT and (2) shungite in styrene–butadiene latex.

For the samples based on shungite, a decrease in the absorption index for the highest concentration is noteworthy. This is repeated on the concentration dependence of the electrical conductivity on the direct current of these composites. For the CNT-based composites, as shown below, the concentration dependence of the dc electrical conductivity differs from the course of the shungite dependences, both the microwave reflection and the microwave absorption, and hence the high-frequency conductivity. The only common aspect in these dependences is the more or less pronounced presence of a critical concentration at the level of 15–20 wt % in the liquid phase or 45–50 wt % in the solid phase. The obtained data on the microwave absorption of the composite protective coatings are of major interest from the point of view of various practical applications. First of all, these are means of individual and collective protection against microwave radiation.

Conclusion

The liquid-phase composite paint coatings based on carbon materials and organic polymer styrene– butadiene latex have been created. The composites allow applying microwave protective coatings using traditional paint and lacquer methods. To produce effective radioprotective coatings, it is required to achieve the maximum content of carbon nanomaterials in composites. A composite with an 80–90% content of carbon nanoparticles in styrene–butadiene latex can be used as a protective coating. The electrical conductivity of composite films is characterized by a complex dependence of the conductivity on the CNT concentration. In the narrow range of concentrations, the effect of stochastic "switching" has been found, which is expressed in abrupt and big changes in the conductivity of the samples, connected with clusters formation. In practical terms, this can be of interest when creating sensor devices and information security systems. Practical interest is presented by the radio-absorbing properties of the studied composites, which are independent of the thickness of the composite layer. One of the promising areas is the protection from microwave radiation of personnel working with microwave appliances, and a variety of electronic devices. Composites based on taunite-M and shungite can be used as radioprotective coatings. Shungite is a natural mineral that is found in very large quantities, while taunite-M has to be obtained expremently. A complex dependence of the morphology of the composite layers on the concentration of CNM in them allows controlling their electrical and radar absorbing properties in a wide range. For this reason, with only two initial components—CNM and a film-forming polymer, one can create a series of composites with significantly different parameters. In the future, composites obtained by directional spinning (threaded) for radioprotective coatings may be of particular interest, wherein fluoroplastic varnish is used as the polymer and wherein up to 95% CNTs can be introduced [59].

References

1. KS Bubarenko, Aprobatsiya (2015), 2: 171–3.

2. Yu A Mikhailin, Nauchn. Osn. Tekhnol (2015) 2: 488.

3. SA Smirnova, Konstr. Kompoz. Mater (2016), 1: 41–50.

4. AI Belous (2015) Space Electronics, Moscow: Tekhnosfera, 488.

5. AV Eletskii, AA Knizhnik, BV Potapkin, and Kh M Kenin, Usp. Fiz. Nauk (2015) 85: 225–70.

6. R Bell, MC Payne, AA Mostofi (2014) Phys. Rev. B, 89: 145426.

7. GJ Panazzi, et al. (2013) J Phys Chem. C, 117, 8020–7.

8. AA Babaev, AM Aliev, PP Khokhlachev, Yu A Nickolaev, EI Terukov, et al. (2016) in Graphene Science Handbook: Size-Dependent Properties, Boca Raton, FL: CRC Press, 5: 505.

9. AA Babaev, AM Aliev, PP Khokhlachev, Yu A Nickolaev, EI Terukov et al. (2016) in Graphene Science Handbook: Size- Dependent Properties, Boca Raton, FL: CRC Press, 5: 505.

10. AA Babaev, PP Khokhlachev, EI Terukov, Yu A Nikolaev, AB Freidin et al. (2015) Phys. Solid State, 57: 424–8.

11. AA Babaev, PP Khokhlachev, KM Aliev, EI Terukov, AK Filippov (2014) Proc. 9th Int. Conference "Amorphous and Microcrystalline Semiconductors", St. Petersburg, 43–5.

12. AA Babaev, PP Khokhlachev, KM Aliev, EI Terukov, AK Filippov (2014) Proc. 17th Int. Interdisciplinary Symposium "Order, Disorder, and the Properties of Oxides" ODPO-17, Rostov-on-Don, 1: 13–16.

13. AA Babaev, PP Khokhlachev, EI Terukov, Yu A Nikolaev, AB Freidin, RA Filippov et al. (2016) Proc. 8th Int. Scientific and Technical Conference "Micro- and Nanotechnologies for Electronics", Nalchik, 262-5.

14. AA Babaev, RK Arslanov PP Khokhlachev, TR Arslanov, AK Filippov, et al. (2015) Int J Mod Phys Appl, 1: 39-44.

15. TR Arslanov, AA Babaev, RK Arslanov, Khokhlachev PP, Terukhov EI, et al. (2014) Appl. Phys. Lett., 105: 203103.

16. AA Babaev, PP Khokhlachev, RK Arslanov, TR Arslanov, A Yu Mollaev, EI Terukov, et al. (2014) Proc. 9th Int. Conference "Amorphous and Microcrystalline Semiconductors", St. Petersburg, 46-8.

17. AA Babaev, PP Khokhlachev, RK Arslanov, TR Arslanov, AYu Mollaev, et al. (2014) Proc. 17th Int. Interdisciplinary Symposium "Order, Disorder, and the Properties of Oxides" ODPO-17, Rostov-on-Don - Moscow, 1: 10-2.

18. TR Arslanov, AA Babaev, RK Arslanov, PP Khokhlachev, EI Terukov et al. (2015) Bull. Rus. Acad. Sci.: Phys, 79: 755–758.

19. AA Babaev, RK Arslanov, PP Khokhlachev, TR Arslanov, EI Terukov , et al. (2015) Proc. Int. Conference "Deformation and Fracture of Materials and Nanomaterials", November 10–13, 2015, Moscow: A. Baikov Institute of Metallurgy and Materials Science Russ Acad Sci, 551–53.

20. AA Babaev, TR Arslanov, PP Khokhlachev, RK Arslanov, EI Terukov et al. (2016) Proc. Int. 8th Scientific and Technical Conference "Micro- and Nanotechnologies for Electronics", Nalchik, 386-9.

21. AA Babaev, AM Aliev, EI Terukov, AK Filippov (2017) High Temp, 55: 502– 5.

22. AA Babaev, AM Aliev, EI Terukov, AK Filippov (2017) Bull. Rus. Acad. Sci.: Phys, 81: 623–5.

23. AA Babaev, AM Aliev, EI Terukov, AK Filippov (2016) Proc. 6th Int.Interdisciplinary Symposium "Physics of Surface Phenomena, Interphase Boundaries and Phase Transitions", Nalchik, Rostov-on-Don, 36.

24. AA Babaev, AM Aliev, EI Terukov, AK Filippov (2016) Proc. Int. Conference "Amorphous and Microcrystalline Semiconductors", St. Petersburg, 47-9.

25. AA Babaev, AM Aliev, EI Terukov, AK Filippov, Izv Vyssh Uchebn Zaved Fiz (2017) 60: 27–30.

26. DA Makeiff, T Huber, P Safille(2005)Defense R&D Canada-Atlantic, Technical Memorandum, DRDC Atlantic TM 2004-124, 20.

27. GP Aleksyuk, VV Shamanin, Yu F Biryulin, EI Terukov, AG Tkachev (2008) Negrov, RF Patent 2325417.

28. LI Rudaya, VV Shamanin, Yu F Biryulin, EI Terukov, AG Tkachev et al. (2009) RF Patent 2373246.

29. AC Dupuis (2005) Prog Mater Sci, 50: 929.

30. EG Rakov (2006) Nanotubes and Fullerenes. Student's Book, Moscow: Logos.

31. DE Resasco, R Kitiyanan, JH Harwell, W Alvarez (2002) US Patent 20020165091.

32. DE Resasco, R Kitiyanan, JH Harwell, W Alvarez (2008) US Patent 20080107588.

33. D Moy, A Chishti (2001) US Patent 20010014307.

34. E Flahaut, A Paigney, Ch Laurent, Ch Marliere, F Cyastel et al. (2000) 48: 3803.

35. J Ma, D Moy (2008) US Patent.

36. DE Resasco (2006) US Patent 20060057055.

37. Q Zyang, W Qian, Q Wen, Y Liu, D Wang, F Wei (2007) Carbon, 45: 1645.

38. AG Tkachev, AV Melezhik, TP D'yachkova, MA Tkachev (2009) RF Patent 2009140251/04.

39. AG Tkachev, AV Melezhik, IV Ivanova (2010) RF Patent 2010124595/04.

40. VA Timofeeva, AB Solov'eva, NA Erina, SS Rozhkov, NF Kedrina (2006) Geology and Mineral Resources of Karelia, Petrozavodsk, 145-55.

41. Yu A Glebova (2016) Extended Abstract of Cand. Sci. (Chem.) Dissertation, Kazan.

42. AN Nurmukhametova (2012) Extended Abstract of Cand. Sci. (Chem.) Dissertation, Kazan.

43. EA Knyachenko (2012) Extended Abstract of Cand. Sci. (Chem.) Dissertation, Kazan.

44. MZ Abdullin, Vestn Kazan (2012) Tekhnol Univ, 11: 118.

45. MF Galikhanov, IF Karimov (2010) Vestn. Kazan. Tekhnol. Univ., 10: 661.

46. OG Shaganov, VV Yanov, LA Zenitova (2016) Vestn. Kazan. Tekhnol. Univ., 19, no. 15: 113.

47. AG Alekseev, EA Shtager, SV Kozyrev (2007) Physical Fundamentals for Stealth Technology, St. Petersburg: VVM, 138.

48. IV Zolotukhin, IM Golev, AS Markova, Yu V Panin, Yu V Sokolov et al. (2006) Tech. Phys. Lett., 32,199-200.

49. AA Babaev, ME Zobov, EI Terukov, AG Tkachev, Zh Tekh Fiz (2010) 90: 430, Tech Phys, 65: 3, 410–3.

50. AA Babaev, ME Zobov, EI Terukov, AG Tkachev (2019) Vestn Dagest Gos Univ, 34: 7.

51. VD Andreev, TA Nachal'naya, Yu I Sozin, VA Semenovich, AF Goncharo, et al. (1991) Proc. 1st Int. Seminar on Diamond Films, Moscow, 18: 1991.

52. AA Babaev, ME Zobov, EI Terukov, AG Tkachev (2020) Prot. Met. Phys. Chem. Surf, 56: 734–9.

53. V Tselik, K Prikhod, A.Raguotis, B Vengalis (1993) Tech Phys Lett, 19: 120.

54. MF Masterov, AV Prikhod'ko, OI Kon'kov, EI Terukov, Fiz Tverd Tela (1997) 39: 31.

55. Terukov EI, Babaev AA, Tkachev AG, Zhilina DV (2018) Tech Phys, 63: 1044– 48.

56. AA Babaev, ME Zobov, EI Terukov, AG Tkachev (2019) Proc. Russian Conference, St. Petersburg, 188.

57. Ravich Yu I, Nemov SA (1995) Amorphous Bodies, Alloys, and Heterogeneous Media, St. Petersburg: Saint-Petersburg State Institute of Technology, 14.

58. SV Demyshev, Yu V Kosichkin, VI Larchev, AG Lyapin, SV Popova (1987) Pis'ma Zh Eksp Teor Fiz, 45: 573.

59. B Bagautdinov, K Ohara, AA Babaev (2022) High-energy X-Ray diffraction study of multiwalled carbon nanotubes fabricated by arc discharge plasma process, Carbon, 1-9.